J Solid State Electrochem (2005) 9: 874–881
DOI 10.1007/s10008-005-0037-3

ORIGINAL PAPER

Galyna Shul · Maria A. Murphy · Geoff D. Wilcox
Frank Marken · Marcin Opallo

Effects of carbon nanofiber composites on electrode processes involving liquid|liquid ion transfer

Received: 29 April 2005 / Revised: 19 May 2005 / Accepted: 14 June 2005 / Published online: 18 August 2005

Abstract Composite electrodes were prepared from chemical vapor deposition grown carbon nanofibers consisting predominantly of ca. 100 nm diameter fibers. A hydrophobic sol–gel matrix based on a methyl-trimethoxysilane precursor was employed and composites formed with carbon nanofiber or carbon nanofiber—carbon particle mixtures (carbon ceramic electrode). Scanning electron microscopy images and electrochemical measurements show that the composite materials exhibit high surface area with some degree of electrolyte solution penetration into the electrode. These electrodes were modified with redox probe solution in 2-nitrophenyloctylether. A second type of composite electrode was prepared by simple pasting of carbon nanofibers and the same solution (carbon paste electrode). For both types of electrodes it is shown that high surface area carbon nanofibers dominate the electrode process and enhance voltammetric currents for the transfer of anions at liquid|liquid phase boundaries presumably by extending the triple-phase boundary. Both anion insertion and cation expulsion processes were observed driven by the electro-oxidation of decamethylferrocene within the organic phase. A stronger current response is observed for the more hydrophobic anions like ClO_4^- or PF_6^- when compared to that for the more hydrophilic anions like F^- and SO_4^{2-}.

Keywords Carbon ceramic electrode · Carbon paste electrode · Carbon nanofibers · Ion transfer · Liquid|liquid interface · Voltammetry

Presented at the 4th Baltic Conference on Electrochemistry, Greifswald, March 13–16, 2005

G. Shul · M. Opallo (✉)
Institute of Physical Chemistry, Polish Academy of Sciences,
ul. Kasprzaka 44/52, 0, 1-224, Warszawa, Poland
E-mail: mopallo@ichf.edu.pl
Fax: +48-22-6311619

M. A. Murphy · G. D. Wilcox
Institute of Polymer Technology and Materials Engineering,
Loughborough University, Loughborough, Leicestershire,
LE11 3TU, UK

F. Marken
Department of Chemistry, University of Bath,
Bath, BA2 7AY, UK

Introduction

The development of composite electrodes modified with organic liquids composed of pure or dissolved redox systems (or ''redox liquids'') recently received a lot of interest [1–3] in particular for applications in ion partitioning analysis [4], photoelectrochemistry at liquid|liquid interfaces [5], and in liquid|liquid electroorganic synthesis [6]. The mechanism of the electrode process involves electron transfer at the electrode|organic liquid interface coupled to a simultaneous ion transfer across the liquid|liquid interface [7, 8]. For unsupported systems, with no supporting electrolyte salt intentionally added into the organic phase, a highly efficient electrode process is observed for the case of close proximity of the electrode surface and both liquid phases, i.e., at the three-phase junction. It has been demonstrated with cylindrical electrodes that the length of this junction is an important factor affecting the efficiency of the overall electrode process [9]. This length can be extended by changing the size and/or number of organic droplets at the electrode surface. It can also be affected by the design of the electrode material affecting the distribution of redox liquid microphases. An electrode composed of electronically conductive (graphite) particles suspended in a hydrophobic silicate matrix (carbon ceramic electrode, CCE) represents the first example [10, 11]. In these electrodes the porous hydrophobic silicate matrix acts as a reservoir for the organic phase and also supports the extended liquid|liquid interface. If the

organic liquid is sufficiently viscous (e.g., for 2-nitrophenyloctylether, NPOE), the use of the silicate backbone can be avoided and a composite electrode formed directly by pasting carbon material with carbon. The electrochemical properties of such carbon paste electrodes (CPEs) are similar to those of redox liquid modified CCEs [12]. Porous silicate films [13, 14], layer-by-layer deposited nanoparticle films [15, 16], or combination of both [17] represent further options for efficient liquid|liquid electrodes. The ''porotrode'' configuration obtained by the deposition of porous layer covered by thin metallic (gold) film exhibits very high efficiency of electrode processes involving redox liquid deposits [18]. The size of conductive particles may affect the efficiency of the electrode process as shown, for example, for CPE systems [12]. In experiments reported here, a high surface area carbon with high porosity—chemical vapour deposition (CVD) grown carbon nanofibers (CNF) with ca. 100 nm diameter—has been chosen as the conducting component of composite electrodes to further improve the characteristics of the liquid|liquid electrodes.

CNFs are formed at ambient pressure by a CVD process employing a nanoparticulate iron catalyst [19] and their electrochemistry has been explored in composites [20], in thin films [21], and grown directly onto ceramic substrates [22, 23]. It has recently been shown by Gong et al. [24] that composite electrodes from carbon nanotubes and sol–gel materials can be prepared by direct deposition onto electrodes. However, we have found the reported procedure of only limited use for CNF immobilization. Here, the preparation, electrochemical properties, and use of different types of CNF-based CCEs and CPEs are described for liquid|liquid redox systems. Anion transfer reactions in aqueous electrolyte solutions employing the decamethylferrocene (DMFc) in NPOE are investigated. CNFs are shown to dominate the electrochemical behaviour of the electrodes and increase the current response for the liquid|liquid anion transfer process.

Experimental

Chemical reagents

Methyltrimethoxysilane (MTMOS) (99%), ferrocenedimethanol (FcDM), and DMFc were obtained from Aldrich; NPOE (99 + %) was obtained from Fluka. NaF, NaSCN, KBr, KCl, KSCN, $KClO_4$, and KNO_3 (analytical grade) were purchased from POCh and KPF_6 (98 + %) from Merck. Graphite powder (MP-300, average particle size 20 μm) was obtained from Carbon GmbH. CNFs were obtained from an ethylene/hydrogen mixture in contact with an iron catalyst following a literature procedure [22]. All chemicals were used without further purification. Water was filtered and demineralized with an ELIX system (Millipore).

Electrode preparation

CCEs were prepared following a procedure described elsewhere [25, 26]. The hydrolyzed sol was prepared by mixing 1 ml of MTMOS with 1.5 ml of methanol. After addition of 50 μl of 11 M HCl it was sonicated for 2 min. Next, 0.17 g of CNFs (or a mixture with carbon particles) was added and further sonicated for 1 min. The resulting paste was immediately placed into a 2 mm deep cavity of a 2 mm inner diameter glass tubing and back-contacted tightly with a copper wire. The electrode was dried at room temperature for at least 48 h and then polished with emery paper. The geometric surface area of the exposed CCE electrode was 0.031 cm^2. CCEs were modified by impregnation with 0.01 mol dm^{-3} DMFc solution in NPOE.

For the CPE preparation 0.17 g of CNFs (or a mixture with graphite powder) was mixed with 100 μl of the redox probe solution in NPOE. The resulting paste was then placed into the 2 mm inner diameter electrode body. The electrode surface was polished with smooth paper. For each voltammetric experiment a freshly modified electrode was employed.

Instrumentation

Cyclic voltammetry (CV) and differential pulse voltammetry (DPV) were performed with an Autolab (Eco Chemie) electrochemical system. The start potential in CV and DPV experiments was always chosen as the most negative point in the potential window. CCEs or CPEs, a platinum wire (diameter 0.5 mm), and an Ag|AgCl|KCl(saturated) were used as the working, counter, and reference electrodes, respectively. The three electrodes were immersed into the aqueous salt solution. All experiments were performed at room temperature (22–23° C). Scanning electron microscopy images were obtained with a Leo 1530 Field Emission Gun Scanning Electron Microscope (FEGSEM) system.

Results and discussion

Characterisation of carbon nanofiber based CCEs

Typical FEGSEM images of CNF-based CCEs prepared with the hydrophobic methyltrimethoxysilane precursor are shown in Fig. 1. It can be seen that a dense network of carbon nanofibers has been formed, stabilized by the ceramic matrix. Particles of hydrophobic silica appear as bright areas with typically 200–500 nm size. It has recently been shown that for carbon particles in the same silica matrix, a much coarser distribution and much more extended silica regions are formed [27]. A closer inspection of this image (see Fig. 1b) reveals the presence of densely packed carbon nanofibers. From the porous structure it can be seen that solvent penetration into the electrode is possible.

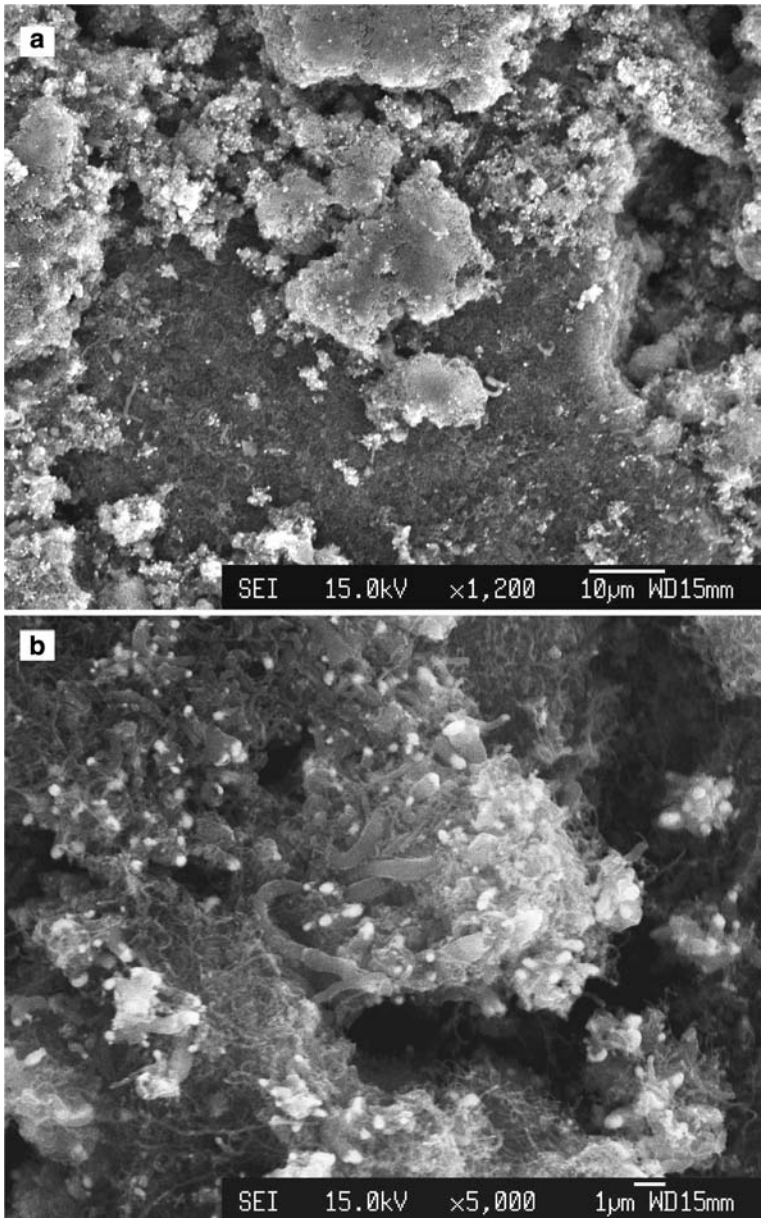

Fig. 1 Typical FEGSEM images of the surface of a ceramic carbon composite electrode composed of CNF and a methyl-trimethoxysilane sol–gel. Two images at lower **a** and higher **b** magnifications are shown

The cyclic voltammograms obtained during continuous scanning of the potential applied to a CNF–CCE immersed in aqueous 0.1 M KNO_3 over a potential window from −0.3 V to +1.0 V versus Ag/AgCl at different scan rates confirm that a high surface area is accessible. Figure 2 shows a comparison of voltammograms obtained with CCE based on a mixture of CNF and graphite particles to that obtained with pure graphite particle based CCE. It is clear that the use of CNF increases approximately four times the magnitude of the capacitive background. It is equal to 75 μF, consistent with 1.2 μg of active CNFs (the capacitance of CNFs is 60 Fg^{-1} [20]) at the electrode surface. For CCEs with a mixture of carbon nanofibers and graphite particles, the CNFs were observed to dominate the capacitive background current. These results indicate that some penetration of the liquid into the porous CNF–CCE structure occurs and an enhanced capacitive background current is observed, but that the electrical contact in the composite material is good and that conventional voltammetric measurements are possible.

Experiments conducted with 1 mM ferrocenedimethanol dissolved in aqueous 0.1 M KNO_3 confirm the well-defined nature of voltammetric responses (Fig. 3). However, the magnitude of the faradaic current is not much affected by the presence of CNF. Well-defined peak currents for both oxidation and reduction processes are observed with a midpoint potential of 0.23 V versus Ag/AgCl. The theoretical peak current for the diffusion-controlled oxidation of the ferrocenedimethanol redox system under these conditions (geometric area = 3.1×10^{-6} m^2, $D = 1\times10^{-9}$ m^2 s^{-1} [19], scan rate = 0.16 Vs^{-1}), $I_p = 10.5$ μA, can be calculated from the appropriate Randles–Sevcik equation [28]. It is

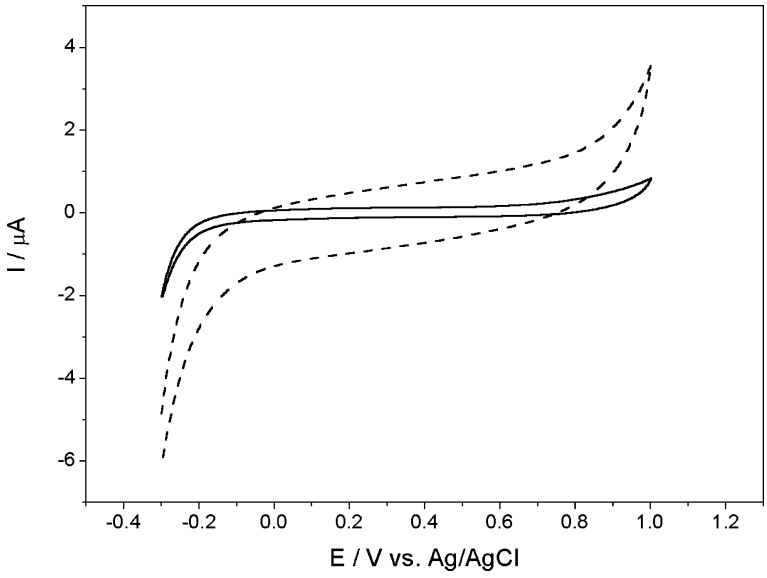

Fig. 2 Cyclic voltammograms (scan rate 0.01 V s^{-1}) obtained with CCE composed of CNF and graphite particles (1:3 ratio) (*dashed*) and only graphite particles (*solid*), immersed in 0.1 mol dm^{-3} aqueous KNO_3

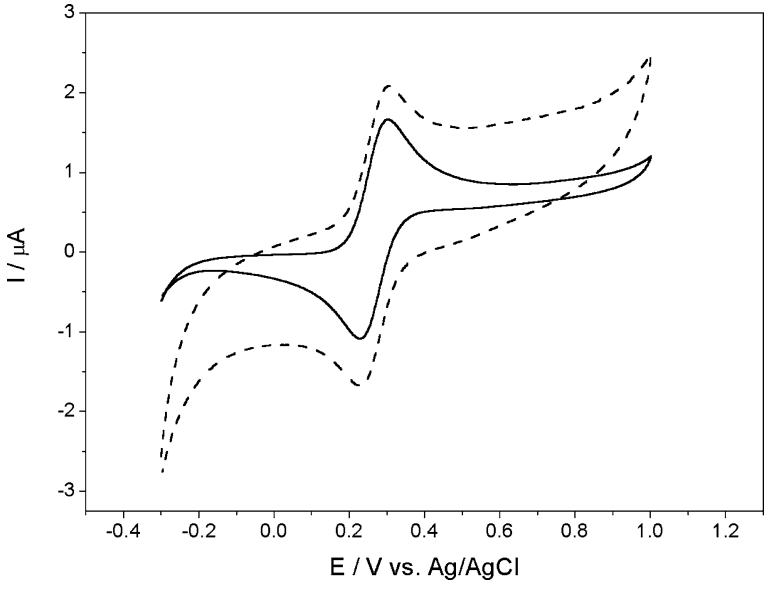

Fig. 3 Cyclic voltammograms (scan rate 0.01 V s^{-1}) obtained with CCE composed of CNF and graphite particles (1:3 ratio) (*dashed*) and only graphite particles (*solid*), immersed in 0.001 mol dm^{-3} ferrocenedimethanol solution in 0.1 mol dm^{-3} aqueous KNO_3

larger than the measured peak current, $I_p = 6.6$ μA, indicating that similar to graphite particles based CCE only a fraction of the electrode surface is electrochemically active. This is consistent with the heterogeneous structure of the electrode. This indicates that the electrical double layer builds up at larger surface not necessarily accessible by the redox probe molecules present in the solution. Further increase of the CNF content leads to the mechanical instability of the electrode material. More benefits from the use of CNF can be seen after modification with redox liquid.

The effect of carbon nanofibers on the electrochemical behaviour of redox liquid modified CCEs and CPEs

Next, CCEs were prepared with pure carbon nanofibers and with a mixture of carbon nanofibers and 20 μm diameter graphite particles. The electrodes were impregnated with a solution of 10 mM decamethylferrocene in NPOE and then immersed into aqueous 0.1 M NaCl electrolyte solution.

The cyclic voltammograms obtained during continuous potential scanning of CCEs made of CNF and/or graphite particles and modified with DMFc solution in NPOE are presented in Fig. 4. The electro-oxidation of the redox probe dissolved in the organic liquid can clearly be observed. Also the effect of the nature of conductive particles on the efficiency of the electrode process can clearly be seen. In the presence of CNFs, significantly higher peak currents are observed. This can be explained with the extended length of the three phase junction electrode|organic liquid|aqueous solution present in the highly porous CNF composite material. Addition of graphite particles did improve the mechanical stability of the electrodes and therefore best

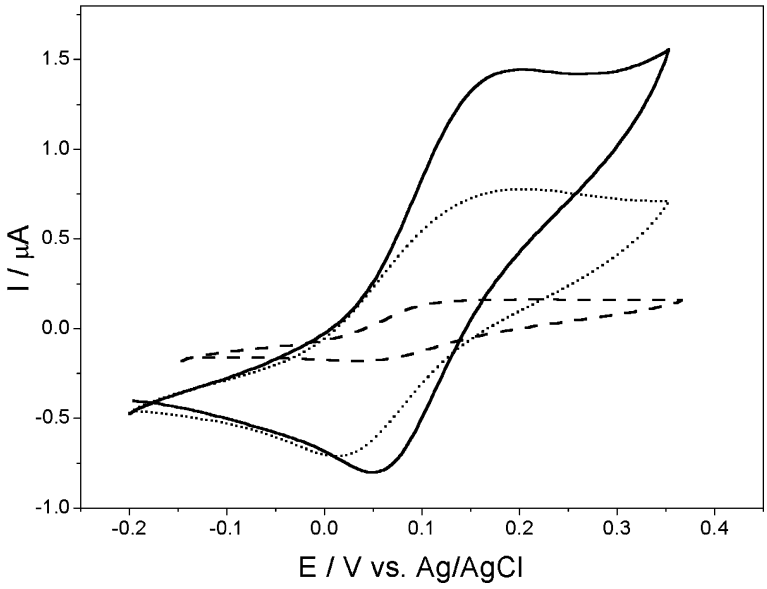

Fig. 4 Cyclic voltammograms (scan rate 0.01 V s^{-1}) obtained with CCE composed of (*solid*) CNF, (*dotted*) CNF and graphite particles (1:3 ratio), and (*dashed*) graphite particles, modified with 0.01 mol dm^{-3} DMFc solution in NPOE immersed in 0.1 mol dm^{-3} aqueous NaCl

results were obtained with ca. 25% CNFs and 75% graphite particles.

A qualitatively similar result is observed with CPEs (see Fig. 5). For electrodes composed of a paste of CNFs and graphite particles in 10 mM decamethylferrocene containing NPOE and immersed in aqueous 0.1 M $NaClO_4$, significant improvements in the peak current in the presence of CNFs are observed. In both the silicate matrix and the paste, the three-phase junction appears to be extended and the CNFs are crucial rather than the silicate [12, 27]. The position of both anodic and cathodic peaks is not significantly affected by the presence of the CNFs. However, the increase of the current during polarization of the CPE towards more positive potentials is observed. The peak-shaped cyclic voltammograms result from the initial electrochemical oxidation of DMFc in the organic phase (Eq. 1).

$$\mathrm{DMFc(org)} \leftrightarrow \mathrm{DMFc^{+}(org)} + e^{-}(\mathrm{electrode}) \qquad (1)$$

This process is initiated at the three phase junction [29, 30] because initially, essentially, no charged species are present in NPOE. For charge neutrality to be maintained ion transfer is required. In order to select one of the two possible pathways (either anion transfer from the aqueous into the organic phase or cation transfer from the organic into the aqueous phase) leading to the neutralization of charge, the experiments were performed in different types of aqueous electrolytes. Both types of electrodes, CCE and CPE, were compared and experiments were performed employing DPV.

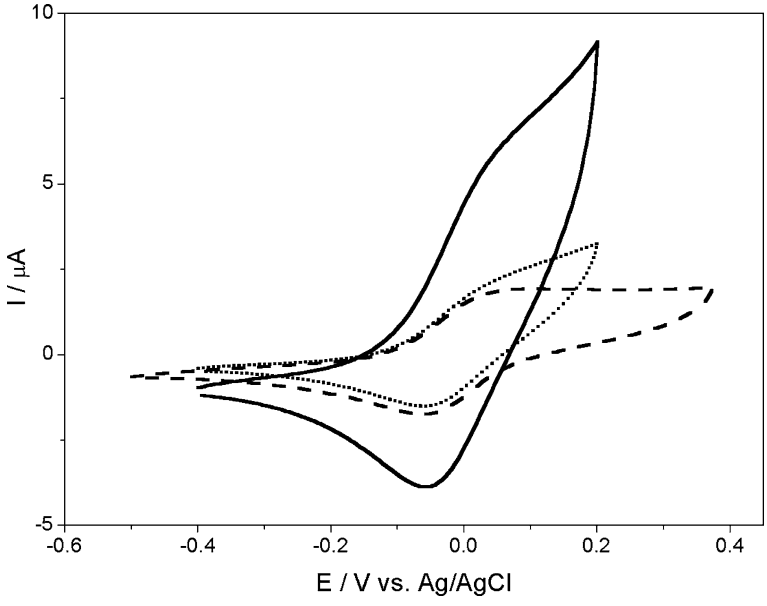

Fig. 5 Cyclic voltammograms (scan rate 0.01 V s^{-1}) obtained with CPE composed of (*solid*) CNF, (*dotted*) CNF and graphite particles (1:3 ratio), and (*dashed*) graphite particles, modified with 0.01 mol dm^{-3} DMFc solution in NPOE immersed in 0.1 mol dm^{-3} aqueous $NaClO_4$

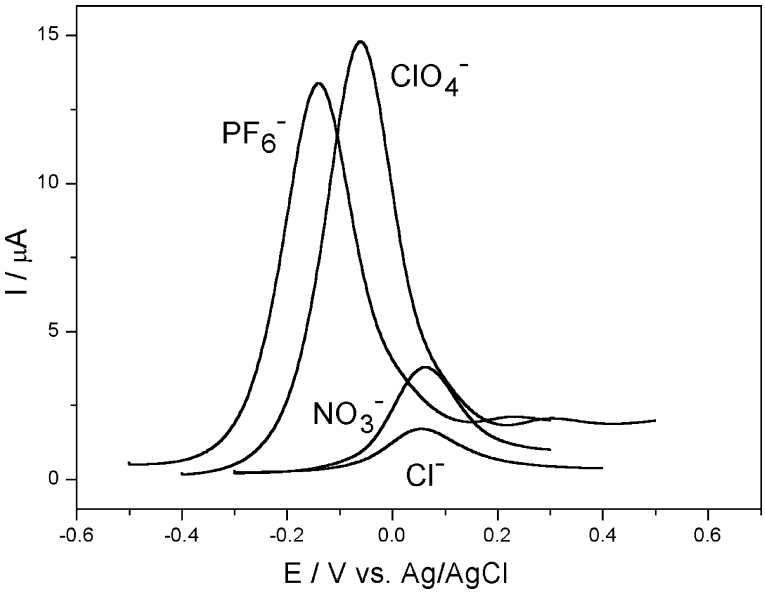

Fig. 6 Differential pulse voltammograms (step potential 0.01 V, modulation amplitude 0.01 V, modulation time 0.05 s, interval time 1 s) obtained with CCE composed of CNF and graphite particles (1:3 ratio) modified with 0.01 mol dm^{-3} DMFc solution in NPOE immersed in 0.1 mol dm^{-3} aqueous solution containing separately: KPF_6, $KClO_4$, KNO_3, and KCl

Liquid|liquid standard transfer potential measurements with carbon nanofiber modified CCEs and CPEs

Typical differential pulse voltammograms obtained at a CCE containing CNFs and impregnated with 10 mM decamethylferrocene containing NPOE are shown in Fig. 6. Various types of electrolyte media were used and it can be seen that anions present in the aqueous phase strongly affect the mechanism of the electrode process. The transfer of anions from the aqueous into the organic phase (assuming that no ion pairing occurs) can be described formally as in Eq. 2.

$$\mathrm{DMFc^+(org) + X^-(aq) \rightarrow DMFc^+(org) + X^-(org)} \tag{2}$$

For the coupled electron- and ion-transfer reaction steps (Eqs. 1 and 2) the midpoint potential ($E_{\mathrm{Red/Ox}}$) is expected to show a Nernstian dependence on the aqueous electrolyte concentration($c_{\mathrm{X^-}}$) [3, 7].

$$E_{\mathrm{Red/Ox}} = E^0_{\mathrm{DMFc^+_{org}/SDMFc_{org}}} + \Delta^{\mathrm{NPOE}}_{\mathrm{aq}}\varphi^0_{\mathrm{X^-}} + \frac{RT}{F}\ln c_{\mathrm{X^-}} + \frac{RT}{F}\ln\frac{c_{\mathrm{DMFc}}}{2} \tag{3}$$

In this expression, $E^0_{\mathrm{DMF^+_{org}/DMFc_{org}}}$ is the standard redox potential for the $DMFc^+$/DMFc couple in the organic solution, $\Delta^{\mathrm{NPOE}}_{\mathrm{aq}}\varphi^0_{\mathrm{X^-}}$ is the standard transfer potential of X^- from water into the NPOE phase, and $c_{\mathrm{X^-}}$ and c_{DMFc} denote initial concentrations of X^- in the aqueous phase and DMFc in the organic phase. If the reaction mechanism is formally given by Eqs. 1 and 2, for measurements with a range of different anions one would expect a linear plot of $E_{\mathrm{Red/Ox}}$versus $\Delta^{\mathrm{NPOE}}_{\mathrm{aq}}\varphi^0_{\mathrm{X^-}}$ with unity slope. Because the value of the latter parameter is known only for limited number of anions and solvents, we used in the data analysis for our results the tabulated value of the standard transfer potential of X^- from water to nitrobenzene($\Delta^{\mathrm{NB}}_{\mathrm{aq}}\varphi^0_{\mathrm{X^-}}$) [31]. This procedure is justified because of the dominant effect of the anion solvation in water.

Figure 7a summarizes voltammetric data for the transfer of anions from aqueous solution into NPOE immobilized in a CCE. Although the points representing $E^0_{\mathrm{DMF^+_{org}/DMFc_{org}}}$ in the presence of most hydrophobic anions are somewhat scattered, the approximately linear dependence on $\Delta^{\mathrm{NB}}_{\mathrm{aq}}\varphi^0_{\mathrm{X^-}}$ with unity slope can be observed (see dashed line). A similar relationship was observed for the droplet of DMFc solution in NPOE deposited on paraffin-impregnated graphite electrode [32] or on graphite composite [27] or carbon paste [12] electrode impregnated with the same solution. By including more data points a line with lower slope (solid line) can be drawn. The deviation of the slope (equal to 0.56 and 0.49 for CCE and CPE electrodes, respectively) from unity, also observed for $E_{\mathrm{Red/Ox}}$versus $\Delta^{\mathrm{NPOE}}_{\mathrm{aq}}\varphi^0_{\mathrm{X^-}}$ [33] (see inset of Fig. 7a, b), is introduced by the more hydrophilic NO_3^-, Br^-, and Cl^- anions and indicate that the contribution from the ejection of electrogenerated $DMFc^+$ cations from the organic phase into the aqueous solution becomes important (Eq. 3).

$$\mathrm{DMFc^+(org) \rightarrow DMFc^+(aq).} \tag{3}$$

This cation transfer process clearly dominates in the presence of more hydrophilic anions like F^- and SO_4^{2-}. Very similar dependences are observed for CCEs and CPEs, which indicates that both types of CNF composite electrodes give quantitatively consistent data. The interpretation of the voltammetric data employing more hydrophobic anions as anion transfer and employing more hydrophilic anions as cation transfer is further corroborated by the shape of the differential pulse voltammograms shown in Fig. 6. For the case of cation

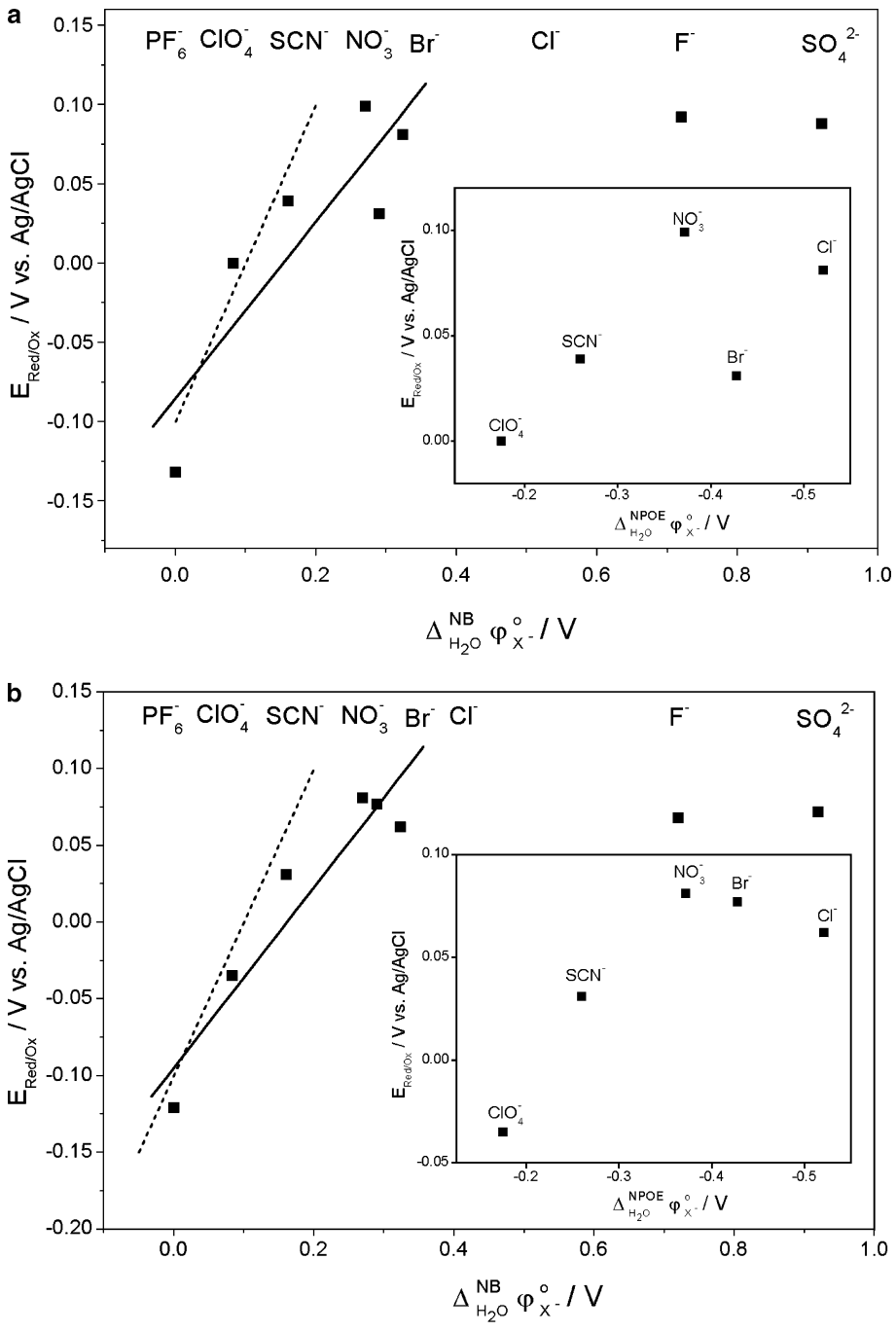

Fig. 7 **a** Plot of the redox potential, $E_{\mathrm{Red/Ox}}$, versus standard transfer potential of anion transfer from aqueous to NB phase, $\Delta_{\mathrm{Aq}}^{\mathrm{NB}}\varphi_{\mathrm{X}^-}^0$. $E_{\mathrm{Red/Ox}}$ values were determined from differential pulse voltammograms with CCE composed of CNF, modified with 0.01 mol dm^{-3} DMFc solution in NPOE and immersed in 0.01 mol dm^{-3} aqueous salt solution. The sequence of anions is indicated on top of the plot. Inset shows analogous plot of $E_{\mathrm{Red/Ox}}$, versus standard transfer potential of anion transfer from aqueous to NPOE phase, $\Delta_{\mathrm{Aq}}^{\mathrm{NPOE}}\varphi_{\mathrm{X}^-}^0$, for selected data of the same system. **b** The redox potential, $E_{\mathrm{Red/Ox}}$, versus standard transfer potential of anion transfer from aqueous to NB phase, $\Delta_{\mathrm{Aq}}^{\mathrm{NB}}\varphi_{\mathrm{X}^-}^0$, plot obtained with CPE composed of CNF and 0.1 mol dm^{-3} DMFc solution in NPOE. $E_{\mathrm{Red/Ox}}$ values were determined from differential pulse voltammograms. The *solid line* indicates unit slope. The sequence of anions is indicated on top of the plot. Inset shows analogous plot of $E_{\mathrm{Red/Ox}}$ versus standard transfer potential of anion transfer from aqueous to NPOE phase, $\Delta_{\mathrm{Aq}}^{\mathrm{NPOE}}\varphi_{\mathrm{X}^-}^0$, for selected data of the same system

expulsion, no build-up of ionic charge carriers in the organic phase occurs and voltammetric signals remain small. However, for the case of the transfer of hydrophobic anions the concentration of ions in the organic phase increases and the reaction zone can extend from the triple-phase boundary into the organic phase. This is probably the reason that much higher current is detected.

Conclusions

CNFs have been incorporated into composite electrodes for use with liquid|liquid redox systems. CNF–CCEs in comparison with conventional graphite particle based CCEs exhibit higher capacitive currents. After modification with a solution of decamethylferrocene in NPOE and immersion into an aqueous electrolyte solution, ion transfer processes can be driven across the liquid|liquid interface. For both CCE and CPE systems, good efficiencies and consistent voltammetric characteristics have been observed. The addition of graphite particles into the CNF–CCE improves the electrode stability.

Acknowledgements This project was partially supported by Polish Committee for Scientific Research (research project 3 T09A 019 26). Also, the support from Polish–British Partnership Programme

sponsored by British Council and Committee for Scientific Research (project WAR/314/248) is gratefully acknowledged.

References

1. Banks CE, Davies TJ, Evans RG, Hignett G, Wain AJ, Lawrence NS, Wadhavan JD, Marken F, Compton RG (2003) Phys Chem Chem Phys 5:4053
2. Scholz F, Gulaboski R (2005) Chem Phys Chem 6:16
3. Scholz F, Schröder U, Gulaboski R (2005) The electrochemistry of immobilised particles and droplets. Springer-Verlag, Berlin, Germany
4. Bouchard G, Galland A, Carrupt PA, Gulaboski R, Mirceski V, Scholz F, Girault HH (2003) Phys Chem Chem Phys 5:3478
5. Wadhawan JD, Compton RG, Marken F, Bull SD, Davies SG (2001) J Solid State Electrochem 5:301
6. Davies TJ, Garner AC, Davies SG, Compton RG (2004) J Electroanal Chem 570:171
7. Marken F, Webster RD, Bull SD, Davies SG (1997) J Electroanal Chem 437:209
8. Scholz F, Komorsky-Lovric S, Lovric M (2001) Electrochem Commun 3:112
9. Bak E, Donten M, Stojek Z (2005) Electrochem Commun 7:483
10. Opallo M, Saczek-Maj M (2001) Electrochem Commun 3:306
11. Opallo M, Saczek-Maj M (2002) Chem Commun 448
12. Shul G, Opallo M (2005) Electrochem Commun 7:194
13. Niedziolka J, Opallo M (2004) Electrochem Commun 6:475
14. Niedziolka J, Nowakowski R, Palys B, Opallo M (2005) J Electroanal Chem 578:239
15. Stott SJ, McKenzie KJ, Mortimer RJ, Hayman CM, Buckley BR, Bulman Page PC, Marken F, Shul G, Opallo M (2004) Anal Chem 76:5364
16. McKenzie KJ, Marken F, Shul G, Opallo M (2005) Farad Discuss 76:5364
17. Niedziolka J, Marken F, Opallo M in preparation
18. McKenzie KJ, Niedziolka J, Paddon CA, Marken F, Rozniecka E, Opallo M (2004) Analyst 129:1181
19. Marken F, Gerrard MI, Mellor IM, Mortimer RJ, Madden CE, Fletcher S, Holt K, Ford JS, Dahm RH, Page F (2001) Electrochem Commun 3:177
20. Van Dijk N, Fletcher S, Madden CE, Marken F (2001) Analyst 126:1878
21. Murphy MA, Wilcox GD, Dahm RH, Marken FM (2005) Indian J Chem 44:924
22. Murphy MA, Wilcox GD, Dahm RH, Marken F (2003) Electrochem Commun 5:51
23. Murphy MA, Marken F, Mocak J (2003) Electrochim Acta 48:3411
24. Gong K, Zhang M, Yan Y, Su L, Mao L, Xiong S, Chen Y (2004) Anal Chem 76:6500
25. Tsionsky M, Gun G, Glezer V, Lev O (1994) Anal Chem 66:1747
26. Rabinovich L, Lev O (2001) Electroanalysis 13:265
27. Shul G, Opallo M, Marken F (2005) Electrochim Acta 50:2315
28. Scholz F (2002) Electroanalytical methods. Springer, Berlin, p 64
29. Schröder U, Compton RG, Marken F, Bull SD, Davies SG, Gilmour S (2001) J Phys Chem B 105:1344
30. Donten M, Stojek Z, Scholz F (2002) Electrochem Commun 4:324
31. http://dcwww.epfl.ch/cgi.bin/LE/DB/InterrDB.pl
32. Gulaboski R, Galland A, Bouchard G, Caban K, Kretschmer A, Carrupt PA, Stojek Z, Girault HH, Scholz F (2004) J Phys Chem B 108:4565
33. Wilke S, Zerihun T (2001) J Electroanal Chem 515:52